Catalysis Today 157 (2010) 183–190

Contents lists available at ScienceDirect

Catalysis Today

journal homepage: www.elsevier.com/locate/cattod

Novel Rh-based structured catalysts for the catalytic partial oxidation of methane

F. Basile[a,b], P. Benito[a,b,*], G. Fornasari[a,b], M. Monti[c], E. Scavetta[c], D. Tonelli[c], A. Vaccari[a,b]

[a] Dipartimento di Chimica Industriale e dei Materiali, ALMA MATER STUDIORUM-Università di Bologna, Viale Risorgimento 4, 40136 Bologna, Italy
[b] Consorzio Interuniversitario per la Scienza e Tecnologia dei Materiali (INSTM), Via Giusti 9, 50121 Firenze, Italy
[c] Dipartimento di Chimica Fisica e Inorganica, ALMA MATER STUDIORUM-Università di Bologna, Viale Risorgimento 4, 40136 Bologna, Italy

ARTICLE INFO

Article history:
Available online 3 June 2010

Keywords:
Electrosynthesis
Metallic foam
Rhodium
Hydrotalcite-type
Catalytic partial oxidation

ABSTRACT

Novel Rh-based structured catalysts were prepared by the electrosynthesis of Rh/Mg/Al hydrotalcite-type (HT) precursors on a FeCrAlY foam. The catalysts obtained by the calcination of HT compounds were investigated in the catalytic partial oxidation (CPO) of CH_4. The effects of the electrosynthesis conditions (potential and pH of the plating solution) on the surface morphology and chemical composition of the samples as well as on the catalytic activity were investigated. The control of the pH of the solution favoured the precipitation of Rh as hydroxide rather than of metallic particles, whereas the potential applied determined the pH value reached near to the foam. By increasing the cathodic potential from −1.2 to −1.3 V, but keeping the synthesis time constant (1000 s), the required conditions to obtain HT precursors were achieved faster and, therefore, a larger amount of them precipitated. Due to the different coverage and chemical nature of the electrosynthesized species, catalytic performances depended on the synthesis conditions, the best values being achieved by the catalyst obtained from the HT precursor prepared at −1.3 V for 1000 s.

1. Introduction

The catalytic partial oxidation (CPO) of methane to syngas ($CO + H_2$) is a slightly exothermic reaction in which high methane conversion and syngas selectivity are achieved at short contact times, making it possible to use small reactors [1–3]. For these reasons, CPO may be used to obtain syngas in small-medium scale plants, i.e. to produce it for distribution. Pelletized catalysts consisting of Ni, Co and noble metals on several supports such as Al_2O_3, $MgAl_2O_4$, CeO_2–ZrO_2 are widely used [4]. However, due to both the high gas-hourly-space-velocity (GHSV) values adopted and the high temperatures reached in the catalytic bed, the mechanical stability of the catalyst and its thermal conductivity play a key role in the development of the process. In this sense, structured catalysts [5] can be useful thanks to their large geometric areas, low pressure drop and high mechanical stability. In addition, by selecting structured supports with high void fractions, thermal conductivity, and convective heat transfer, both the formation of hot spots and the "run away" of the reaction may be avoided [6], as the large amount of heat generated on the upper part of the catalytic bed can be diffused by the metallic support and consumed by further reforming reactions [7].

Bulk metal structured catalysts, such as noble metal gauzes or sponges [8–10] and nickel foams [11,12] have been applied in CPO, although they show low surface area values. On the other hand, structured catalysts in which the active catalyst is deposited on a ceramic or metallic support – such as alumina foams [13–19], extruded cordierite or α-alumina honeycomb monoliths [9,20–26], felts [27], FeCrAlloy and Nicrofer metallic monoliths [28–30] as well as a FeCrAlloy metallic foam [31] - lead to a significant reduction of the amount of catalyst, without a decline in the catalytic performances. In structured catalysts, the amount and dispersion of the active phase can be controlled by changing either the thickness of the coating or the metal loading. Furthermore, the performance of the catalyst is determined by the synthesis procedure, morphology and stability of the film. Different synthetic procedures have been used to coat the supports and obtain CPO catalysts: (i) impregnation or coprecipitation of the salts of the active metals (Rh, Pt or Ni) on alumina-structured supports [15,18,19,22] or impregnation of the elements to form $Zr_{0.8}Ce_{0.2}O_2$ and $LaNi_{0.9}Pt_{0.1}O_x$ phases [26]; (ii) wash-coating of a primer and subsequent impregnation or coprecipitation of the active phase [9,17,20,25]; (iii) wash-coating of a ready made catalyst [27]; (iv) microwave-assisted combustion synthesis of Pt nanoparticles on Al_2O_3 foams [32]. The coating of metallic supports with a ceramic catalyst is not straightforward, since the adhesion of the layer to the support is low and problems can arise during drying and calcination; therefore, the major challenge is in achieving a homogeneous and well-adhered catalyst layer on the monolith walls [33]. In some cases it has been reported that the addition of a primer or the treatment of the sup-

* Corresponding author at: Dipartimento di Chimica Industriale e dei Materiali, ALMA MATER STUDIORUM-Università di Bologna, Viale Risorgimento 4, 40136 Bologna, Italy. Tel.: +39 0512093677; fax: +39 0512093679.
E-mail address: pbenito@ms.fci.unibo.it (P. Benito).

0920-5861/$ – see front matter © 2010 Elsevier B.V. All rights reserved.
doi:10.1016/j.cattod.2010.04.039

port at a high temperature in an oxidizing atmosphere improve the adherence of the catalyst to the support [34,35].

The electrodeposition can be used to deposit hydroxides and/or oxides on metallic supports through the base-electrogeneration method, which consists of the generation of a basic pH near the support by the reduction of an easily reducible anion, like NO_3^- or ClO_4^- [36,37]. This technique, largely used for the preparation of modified electrodes, has been extended to the preparation of catalysts [38–40]. Recently, some of the authors proposed the electrosynthesis and deposition of hydrotalcite (HT)-type compounds, precursors of Ni-based catalysts active in the steam methane reforming [41–43]. HT compounds are layered materials [44,45] that, after calcination, lead to mixed oxides with the active phase well distributed and after reduction small and stable metallic particles are obtained. In particular, HT compounds containing Ni, Co and noble metals have been used as precursors for the CPO of methane [46,47]. In the present study, the base-electrogeneration method has been extended to the preparation of Rh/Mg/Al HT compounds on a FeCrAlY alloy foam, which are precursors of Rh-based catalysts for the CPO of methane [48]. The effects of the pH of the plating solution and potential applied on both the coating properties and the catalytic activity are investigated. Moreover, the aim of this work was to compare the activity of the electrosynthesized catalysts with that of a Rh-based pelletized catalyst with the same structure, it means, obtained from HT compounds.

2. Experimental

2.1. Synthesis of the catalysts

Rh/Mg/Al-NO_3 HT compounds were electrosynthesized on a FeCrAlY foam by cathodic reduction of a solution containing metal salts and KNO_3. The Rh/Mg/Al atomic ratio in the solution was 11/70/19, with a total concentration of 0.03 M. The synthesis was performed at two different pH values of the plating solution: (i) 2.1 that corresponds to the pH obtained by adding nitrates to water and (ii) by adjusting the pH with NaOH to 3.8. Electrochemical deposition was carried out at room temperature (r.t.) using a single compartment, three-electrode cell. Electrode potentials were measured with respect to an aqueous saturated calomel electrode [SCE; i.e. reference electrode (R.E.)]. A Pt gauze was used as counter electrode (C.E.). The working electrode (W.E.) was the FeCrAlY foam (80 ppi and 5% nominal relative density). FeCrAlY foam pellets were obtained by cutting cylinders of 8 mm diameter and 10 mm long from a panel. Electrochemical tests were recorded using a CH instrument Mod. 660 C controlled by a personal computer via CH Instrument software. Electrosynthesis was carried out at two different potentials −1.2 and −1.3 V *vs* SCE for 1000 s. The precursors were named as follows: RhHT-*X*, where *X* = potential applied (−1.2, −1.3). When the pH of the plating solution was controlled at 3.8 the label "pH" was added at the end of the name (e.g. RhHT-1.2pH). Electrosynthesis in the same conditions was also carried out on FeCrAlloy plates to allow a complete characterization of the deposited material. After electrodeposition, the films were gently rinsed with double-distilled water and then dried. The catalysts were obtained by calcination at 900 °C for 12 h of coated foam pellets. The catalysts were named by replacing HT by exHT in the label (e.g. RhexHT-1.2pH). For comparison purposes, a low loaded Rh-based powder catalyst was also prepared by calcination of a HT precursor Rh/Mg/Al (0.1/80/19.9 atomic ratio) containing silicates in the interlayer region; further details on the synthesis are reported elsewhere [49]. The amount of Rh was ca. 0.2 wt.%.

2.2. Characterization techniques

X-ray diffraction (XRD) patterns were collected with Cu Kα radiation (λ = 1.5418 Å) by means of a X'PertPro PANalytical diffractometer equipped with a fast X'Celerator detector. The 3–80° 2θ range was measured performing steps of 0.07° (2θ) and counting 120 s/step. The analyses were performed on a powder that was gently removed from a FeCrAlloy plate. A "zero background" sample holder (The Gem Dugout, State College, PA, USA) was used. Temperature Programmed Reduction and Oxidation (TPR/O) analyses were carried out with a H_2/Ar or an O_2/He (5/95 v/v) gas mixture, respectively (total flow rate 1.2 L/h) in the 100–950 °C temperature range by using ThermoQuest CE Instruments TPDRO 1100. Covered metallic foam pellets were used directly for measurements. SEM/EDS analyses were performed by using an EVO 50 Series Instrument (LEO ZEISS) equipped with an INCAEnergy 350 EDS micro-analysis system and an INCASmartMap for imaging the spatial variation of elements in a sample (Oxford Instruments Analytical). The accelerating voltage was 25 kV, the beam current 1.5 nA, and the spectra collection time 100 s. Specific surface area measurements were carried out in a Micromeritics ASAP 2020 instrument by N_2 adsorption/desorption at −196 °C. The values are given with respect to the total weight of the structured catalyst (foam + catalyst). Samples were previously degassed under vacuum, heated up to 200 °C and maintained at this temperature for 30 min.

2.3. Catalytic tests

Catalytic tests were carried out in a quartz reactor (i.d. 8 mm) operating at atmospheric pressure. Two cylinders of the foams (8 mm × 10 mm) were loaded in the isothermal zone of the reactor. The foams fit well with the diameter of the reactor to minimize any by-pass. Catalysts were reduced in situ before the tests in an equimolar H_2/N_2 mixture (7.0 L/h) for 2 h at 500 °C for the RhexHT-1.2 catalyst and at 750 °C for the RhexHT-1.2pH and RhexHT-1.3pH catalysts. Catalytic tests were performed keeping the temperature of the oven (T_{oven}) constant at 750 and 500 °C and allowing the temperature of the catalyst to vary depending on the endothermicity/exothermicity of the process. The effect of the GHSV values and the concentration of the gas mixture was studied: GHSV = 28,000 and 120,000 h^{-1} (calculated on the total volume of the foam support) and CH_4/O_2/He = 2/1/20 and 2/1/4 (v/v). No large pressure drop was observed during the tests. The catalytic activity of the coated foam pellets was compared with that of a Rh-based pelletized catalyst (average size 600 μm). The tests were performed loading the same weight of the pelletized catalyst than that of the coated foam and feeding the same flow of reactants, keeping therefore the flow/weight (F/W) ($cm^3/g\,h$) constant. The gas phase temperature was measured by a moveable chromel–alumel thermocouple sliding in a quartz wire inside the catalytic bed. The maximum temperature (T_{max}) and that at the outlet of the catalytic bed (T_{out}) were measured. The reaction products were analysed online after water condensation by a PerkinElmer Autosystem XL gas chromatograph, equipped with two thermal conductivity detectors (TCD) and two Carbosphere columns using He as the carrier gas for the analysis of CH_4, O_2, CO and CO_2 and N_2 for the H_2 analysis.

3. Results and discussion

3.1. Characterization

As previously reported for Ni/Al electrosynthesized HT precursors on metallic foams [43], no blockage of the pores occurs. SEM images of the sample prepared at −1.2 V in 1000 s without adjusting the pH of the plating solution, pH = 2.1, indicate that the sample is rather inhomogeneous, as also observed by a visual inspection of the foams. During the electrosynthesis, the whole or a part of the foam turns black, instead of the yellow colour characteristic of Rh^{3+}, pointing out its reduction to Rh^0. A SEM image of some

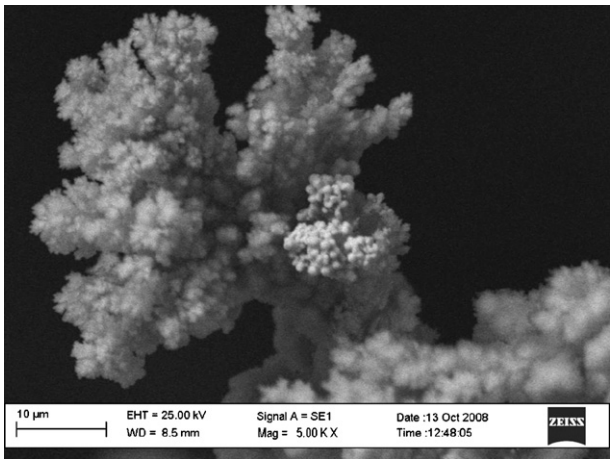

Fig. 1. SEM image of the RhHT-1.2 sample prepared at −1.2 V for 1000 s without adjusting the pH of the nitrate solution (pH = 2.1).

parts of the foam shows the formation of arrays of rounded particles (Fig. 1) and the EDS analysis reveals that they are composed of Rh and Al, while no Mg is detected. In other parts of the foam pellets, the coating is made up of small particles containing Rh, Mg and Al. After calcination several cracks develop. In order to explain the Rh^{3+} to Rh^0 reduction process, some considerations must be taken into account. During the application of a cathodic potential to the solution containing nitrates, a series of reactions takes place, yielding H^+ consumption (Eqs. (1)–(4)) and OH^- generation, mainly by nitrate reduction (Eqs. (5)–(7)). A fast and steady increase in the pH value near the working electrode occurs, leading to the precipitation of hydroxides on the foam surface. The pH close to the surface of the foam depends on the applied potential: for instance, at −1.2 V the pH values range between 8.7 and 9.6 [43].

$$H^+ + e^- \rightarrow H_{ads} \quad \text{or} \quad H_{abs} \tag{1}$$

$$2H^+ + 2e^- \rightarrow H_2 \quad E^\circ = 0.0\,V \tag{2}$$

$$NO_3^- + 2H^+ + 2e^- \rightarrow NO_2^- + H_2O \quad E^\circ = 0.934\,V \tag{3}$$

$$NO_3^- + 10H^+ + 8e^- \rightarrow NH_4^+ + 3H_2O \quad E^\circ = 0.36\,V \tag{4}$$

$$2H_2O + 2e^- \rightarrow H_2 + 2OH^- \quad E^\circ = -0.828\,V \tag{5}$$

$$NO_3^- + H_2O + 2e^- \rightarrow NO_2^- + 2OH^- \quad E^\circ = 0.01\,V \tag{6}$$

$$NO_3^- + 7H_2O + 8e^- \rightarrow NH_4^+ + 10OH^- \quad E^\circ = -0.12\,V \tag{7}$$

Besides, the cation reduction to metal may be competitive with the hydroxide precipitation:

$$Me^{n+} + ne^- \rightarrow Me^0 \tag{8}$$

The nitrate reductions (Eqs. (6) and (7)) have a more positive E° value if compared to most cation reduction reactions [37]. Consequently, the cation deposits in the form of hydroxide on the cathode as previously observed for Ni/Al HT phases [50]. However, the reduction to metal (Eq. (8)) may become competitive for easily reducible metals, for example Rh^{3+} ions; in fact, in acid solutions the formal potential of Rh reduction is 0.76 V, but it decreases when increasing the pH of the solution according to the Pourbaix's diagram [51]. It can therefore be hypothesized that the application of a potential of −1.2 V to the plating solution at its spontaneous pH (pH = 2.1), leads to the precipitation of different phases, due to the formation of potential gradients within the foam, also leading to pH gradients. In particular, it is clear that these experimental conditions do not ensure, at least in some zones of the foam pellet, a sufficiently basic pH to avoid the Rh^0 precipitation and the aluminium hydroxide precipitates as well [43]. In order to suppress the reduction of Rh^{3+} cations, the pH of the solution was adjusted before the experiments to a value of 3.8, the highest possible to avoid $Al(OH)_3$ bulk precipitation.

SEM images of the sample prepared at −1.2 V in 1000 s at pH = 3.8 show a coverage that is not uniform (Fig. 2): uncoated or partially coated zones are observed on the flat surfaces of the foam (Fig. 2b) and a larger amount of solid is observed on its tips (Fig. 2a). Inspection of the sample at higher magnifications reveals that the coating is made up of small particles. The composition

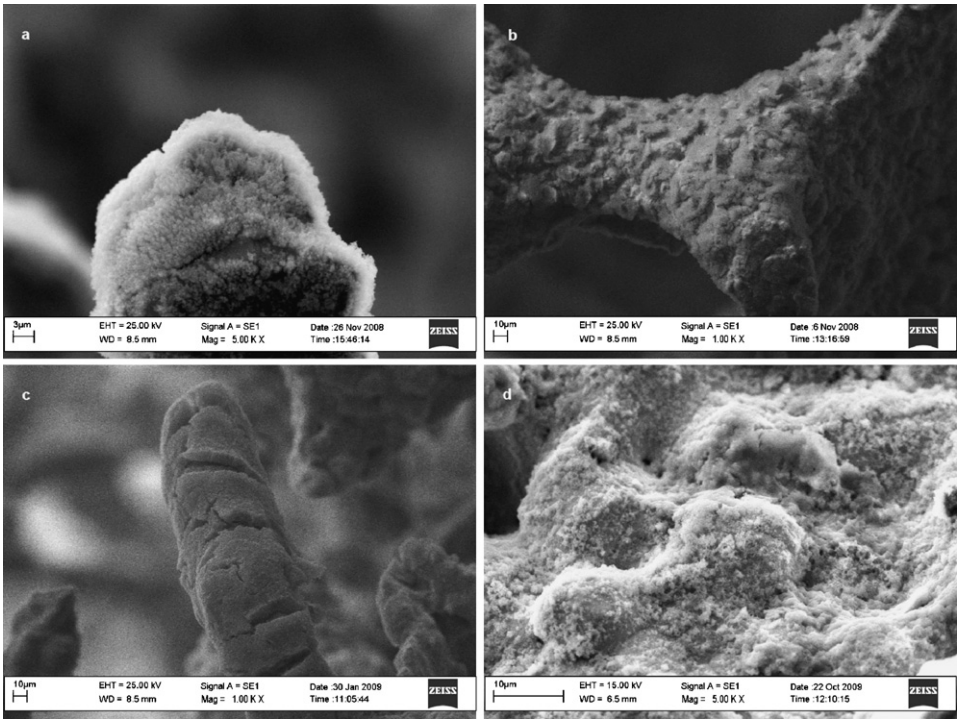

Fig. 2. SEM images of the RhHT-1.2pH and RhHT-1.3pH samples prepared at −1.2 V (a and b) and −1.3 V (c and d) *vs* SCE for 1000 s, by adjusting the pH at 3.8.

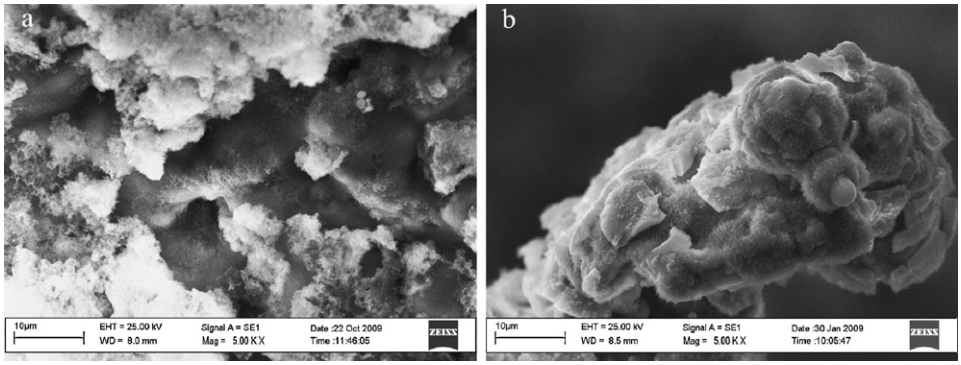

Fig. 3. SEM images of the RhexHT-1.2pH (a) and RhexHT-1.3pH (b) catalysts obtained by calcination of the samples prepared at pH = 3.8 for 1000 s at −1.2 V and −1.3 V, respectively.

of the deposited solid (qualitatively obtained by EDS) is also not homogenous, but the trend in the values is related to the surface coverage. On the flat surfaces of the foam the amounts of Rh and Al (as atomic ratio) are larger than the expected quantities, while the Mg-content is lower. On the other hand, where the thickness of the solid is larger, the solid appears enriched in Mg with a M^{2+}/M^{3+} atomic ratio >3 (instead of 3.0). After calcination (Fig. 3a), the morphology of the solid does not change to a great extent, but some uncovered zones where alumina, coming from the oxidation of the FeCrAlloy foam [52], grows are observed. Considering the weight loss, ca. 40–50% observed for the HT precursors during the calcination, due to the removal of CO_2, H_2O and NO_2, and the formation of compact oxides, the shrinkage may be responsible for the formation of cracks. The differences in thermal expansion coefficients of the ceramic and metallic materials may also be considered. Calcination however may favour the adhesion of the wash-coat to the support, because of the reaction between alumina from the support and the cations of the exHT layer.

When a higher cathodic potential (−1.3 V *vs* SCE) is applied to the metal solution at pH 3.8, the pH increases faster and higher values are obtained (pH = 9.7–11.0), with a higher amount of precipitate. A thick layer is deposited on the surface of the most exposed foam parts (Fig. 2c) and a thin layer coats the support on the flat surfaces (Fig. 2d). The chemical composition of the film is closer to that of the plating solution. It should be noted, however, that some cracks are present in the thicker layers (Fig. 2c), which may be related to: (i) the formation of H_2 bubbles (Eq. (2)) during the synthesis on the foam surface as the applied potential increases; (ii) the drying of the HT phase; (iii) the shearing stresses between the support and the deposit [53]. After calcination, coatings exhibit an arrangement of flakes and interconnected surface cracks (Fig. 3b) that may be related to a shrinkage mechanism as previously reported. The morphology and size of the particles are similar regardless of the potential applied. In the initial stage, nucleation and particles growth compete with each other. The nucleation reaction rate may be high and exceed that of particle growth [53], justifying the similar sizes of the particles. The deposition of small particles would also increase their adhesion to the substrate [54].

In order to obtain structural information about the phases formed during the electrodeposition and after calcination, the syntheses at pH = 3.8 were performed on FeCrAlloy plates and the electrodeposited powder was scratched and analyzed by XRD as-prepared and after calcination at 900 °C (Fig. 4) [43]. XRD patterns of the powders synthesized at both potentials show broad and low intense diffraction lines, characteristic of poorly crystallized HT compounds, together with sharper lines due to a side brucite ($Mg(OH)_2$) phase. After calcination, MgO and spinel-type ($MgAl_2O_4$ and $MgAlRhO_4$) phases are identified. The formation of the $MgAlRhO_4$ phase, not observed in catalysts obtained from HT compounds was related to the high content of Rh in the catalysts

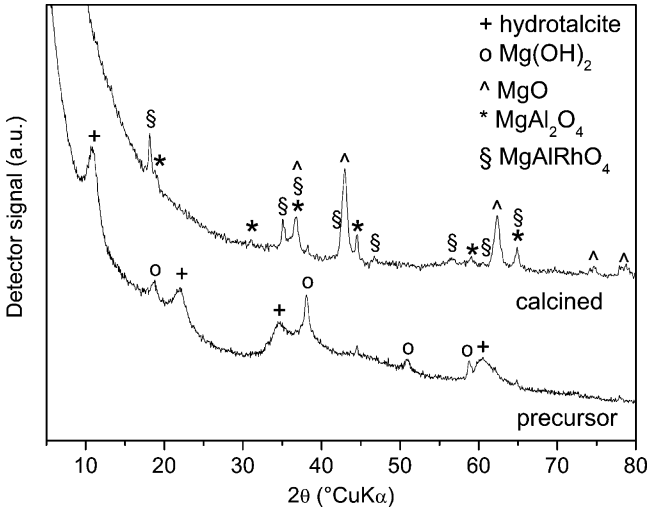

Fig. 4. PXRD patterns of the powder of the precursor prepared at −1.3 V for 1000 s and the catalyst obtained by calcination at 900 °C.

[48]. It should be remarked that in this way the possible reaction between the cations of the HT and the alumina from the oxidation of the foam is neglected, therefore the actual oxide/spinel ratio may be modified.

Temperature Programmed Reduction (TPR) and Oxidation (TPO) analyses of the coated foams were performed (Fig. 5). Two different behaviours are observed in the TPR profiles depending on the pH of the plating solution. The catalyst prepared at a pH value of the plating solution of 2.1 is formed by Rh^{3+} species which are easily reducible. A single H_2 consumption with maximum at approximately 200 °C is observed. The reduction temperature is similar to that reported for rhodium oxide species low interacting with alumina [55] in agreement with EDS data. Furthermore, when the TPR is repeated after the oxidation step, the reduction peak shifts to a lower temperature, pointing to a sintering of the particles. Conversely, catalysts prepared at −1.2 and −1.3 V adjusting to 3.8 the initial pH, show the characteristic profiles of well stabilized Rh-containing particles [48,49], with a H_2 consumption with maximum at ca. 550 °C and a shoulder at lower temperature, together with a rather complex reduction at temperatures above 700 °C. Temperature Programmed Oxidation (TPO) profiles of the RhexHT-1.2pH and RhexHT-1.3pH catalysts (Fig. 5) show a broad O_2 consumption peak at 400 °C related to the oxidation of Rh^0. During the second TPR after the TPO run, a broad H_2 consumption is recorded; however, its low intensity in comparison to that observed for the fresh catalyst could indicate that most of the Rh^0 particles were not oxidized or that difficult-to-reduce species are formed during the oxidation treatment.

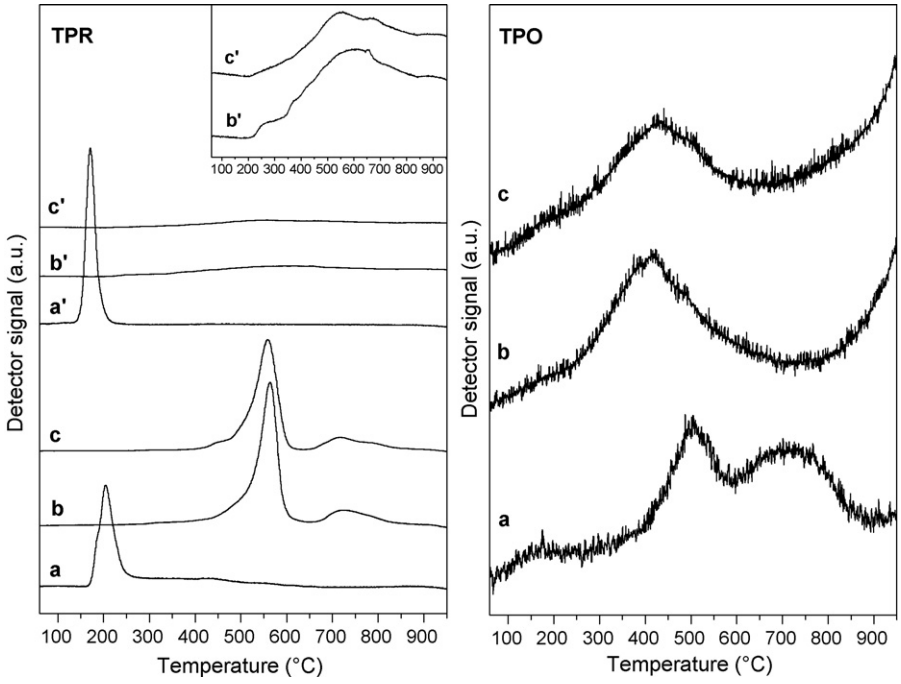

Fig. 5. TPR and TPO profiles of catalysts obtained from Rh/Mg/Al HT precursors electrosynthesized at: −1.2 V for 1000 s without adjusting the pH of the plating solution (a); at −1.2 V (b) and −1.3 V (c) for 1000 s adjusting the pH of the plating solution. In the TPR graph: a′, b′ and c′ refer to the second reduction.

The specific surface area values of the catalysts depend on the synthesis conditions: the RhexHT-1.2pH catalyst do not show any measurable area, whereas for the RhexHT-1.2 and RhexHT-1.3pH samples they range from 0.5 to 1.0 $m^2 g^{-1}$. These low values are related to the small amount of deposited catalyst due to the low thickness of the catalyst layer obtained.

3.2. Catalytic activity

The effect of both the GHSV values (28,000 and 120,000 h^{-1}) and feed mixture concentrations ($CH_4/O_2/He$ = 2/1/4 and 2/1/20, v/v) on the catalytic performances was investigated (Fig. 6). Blank tests were performed with two bare metal foam pellets, observing a low CH_4 conversion to CO, H_2, CO_2 and H_2O during the tests at

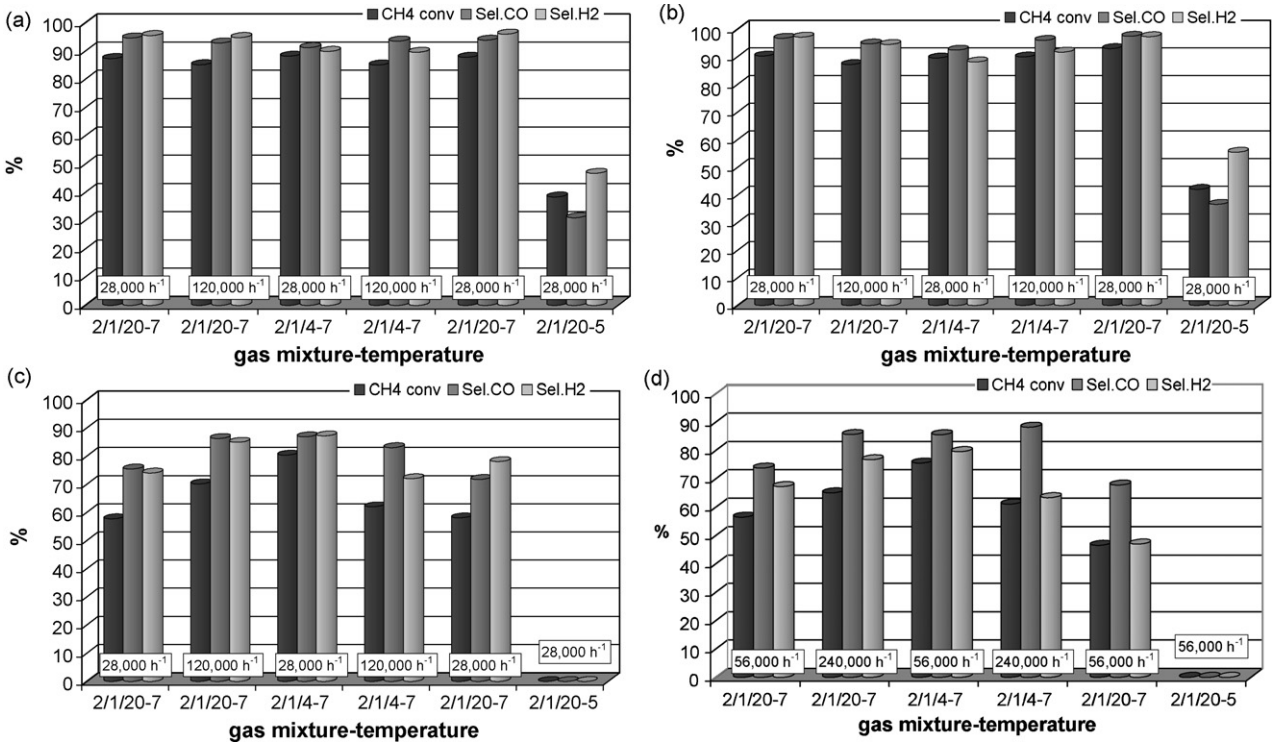

Fig. 6. Catalytic performances of the catalysts tested in the CPO of CH_4, feeding different gas mixtures ($CH_4/O_2/He$ = 2/1/20 and 2/1/4 (v/v)), changing the GHSV values (28,000 and 120,000 h^{-1}) and the oven temperature (7 = 750 °C and 5 = 500 °C). (a) RhexHT-1.2; (b) RhexHT-1.3pH; (c) RhexHT-1.2pH; (d) RhexHT-1.3pH, loading 1 foam pellet (GHSV = 56,000 h^{-1} and 240,000 h^{-1}).

Table 1
Catalytic performances of the pelletized Rh-based catalyst (Rh/Mg/Al = 0.1/80/19.9 atomic ratio) calcined at 900 °C.

$CH_4/O_2/He$ (v/v)	T_{oven} (°C)	F/W ($cm^3/g\,h$)	T_{max} (°C)	T_{out} (°C)	CH_4 conv. (%)	CO sel. (%)	H_2 sel. (%)
2/1/20	750	112,000	802	764	65	81	78
2/1/20	750	470,000	919	866	70	89	78
2/1/4	750	112,000	864	793	84	90	82
2/1/20	750	112,000	792	757	80	92	91
2/1/20	500	112,000	602	572	41	37	51

28,000 h^{-1} with the most concentrated gas mixture. CPO mechanism can be described as an initial exothermic process where oxygen conversion takes place, followed by a reforming zone where steam reforming (SR) together with water gas shift (WGS) reactions occur [56,57]. In the oxidation zone CO, H_2 and H_2O, besides small amounts of CO_2, are formed, whereas in the endothermic zone more CO and H_2 are obtained.

Catalytic data indicate that the best catalytic performances (CH_4 > 85% and syngas selectivity ∼ 90%) were observed over RhexHT-1.2 (Fig. 6a) and RhexHT-1.3pH (Fig. 6b) catalysts. As the GHSV value increases, the CH_4 conversion slightly decreases both in diluted and concentrated tests. Some changes in the CO/H_2 ratio are observed in the concentrated tests, which may be related to the contribution of the reverse WGS, favoured by the temperature increase. In order to check the stability of the catalysts, at the end, the test feeding the diluted gas mixture (2/1/20, v/v) at 28,000 h^{-1} was repeated. No decrease in CH_4 conversion and syngas selectivity is observed, pointing out that both catalysts are stable with time-on-stream. The high temperatures reached in the catalytic bed smooth the differences in activity and move the reaction towards the thermodynamic equilibrium [58]. Therefore, in order to highlight the differences between the catalysts, a test was carried out under conditions far from those of the thermodynamic equilibrium at T_{oven} = 500 °C and feeding the 2/1/20 (v/v) gas mixture [58]. Under these conditions, the heat originated from exothermic reactions is reduced and the thermal conductivity of the gas increased, allowing to study the actual activity and discriminate among catalysts. CH_4 conversion values of 38 and 42% are obtained for samples prepared at −1.2 and −1.3 V, respectively. Moreover, a higher selectivity in H_2 than in CO is obtained, related to the contribution of the WGS reaction [59]. These results indicate that the sample prepared at −1.3 V is slightly more active.

The catalyst obtained from the HT precursor prepared at −1.2 V and by adjusting the initial pH to 3.8 shows poorer performances (Fig. 6c), but O_2 conversion was always complete, with a different trend as a function of the test conditions. By feeding the diluted gas mixture (2/1/20, v/v), the CH_4 conversion improves as the GHSV increases. A further increase of the CH_4 conversion is obtained feeding the concentrated 2/1/4 (v/v) mixture at 28,000 h^{-1}, but unlike for diluted tests, the increase of the GHSV value yields to a decrease of the performances and the catalyst steadily deactivates (the conversion of CH_4 decreases from 76% to 62% in 2 h of time-on-stream). Moreover, the selectivity in H_2 decreases, while selectivity in CO remains almost constant. Similar results were previously obtained by some of us during CPO tests at very short contact time using a similar Rh/Mg/Al bulk catalyst (1/71/28 atomic ratio), where H_2 selectivity decreases at low contact time after a maximum [60]. The behaviour here observed for the H_2 selectivity and CH_4 conversion was attributed to the suppression of SR [16,20,24,25] and/or WGS [60] reactions. It seems that the available Rh^0 active sites are not sufficient to significantly convert CH_4 in the gas mixture. The same methane conversion is obtained in the return tests; while no activity is registered during the tests at a T_{oven} of 500 °C.

To further reduce the contact time, keeping the feed flow rate constant, tests were carried out with a single RhexHT-1.3pH foam pellet (Fig. 6d). By this way, unlike in the experiments reported above, similar heat and mass-transfer characteristics are achieved in the tests [12]. The CH_4 conversion and syngas selectivity follow the same trend observed for the catalyst obtained from the HT compound prepared at −1.2 V for 1000 s, but the activity is reduced, providing that the consumption of CH_4 by steam reforming is too low to go to completion, and a larger amount of catalyst is required to obtain better catalytic performances.

Catalytic performances of a low loaded Rh-based pelletized catalyst are summarized in Table 1. The activity is low during the initial test by feeding the 2/1/20 (v/v) gas mixture; whereas as the space velocity increases or the concentrated gas mixture is fed, higher CH_4 conversion and syngas selectivity are achieved. The improvement of the performances is accompanied by an increase in the gas phase temperature, due to the higher amount of reactants fed and the concentration of the gas mixture [58,61]. The test with the 2/1/4 (v/v) gas mixture at the highest space velocity value was not performed because of temperatures above 1000 °C. In the return tests the activity increases, therefore, it may be stated that during the tests at higher space velocity and/or feeding more concentrated gas mixtures, the catalyst is further reduced due to the high reducing power of the gas mixture, achieving therefore better performances. Finally, by lowering the oven temperature the performances are close to that obtained with the catalyst prepared at −1.3 V. From these results it could be hypothesized that a similar activation has taken place for the RhexHT-1.2pH catalyst. By feeding the 2/1/20 (v/v) gas mixture at 120,000 h^{-1} and the 2/1/4 (v/v) gas mixture at 28,000 h^{-1}, since conversion values are quite similar to those obtained with the pelletized catalyst and considering that the flow rate of reactants was kept constant, a similar increase in the average temperature within the catalytic bed to that reported in Table 1 is expected (even though the thermal profile could be different because of the different type of the catalyst). The high temperature could both activate the catalyst and enhance the conversion values. This activation is not observed during the return tests for the RhexHT-1.2pH catalyst since the catalyst deactivates in the hardest conditions. The pore diameter of the foam and pelletized bed as well as the nature of the support are different, thus they show different mass and heat transfer properties. A comparison of the catalytic performances of the electrochemically prepared foams with foams coated with HT compounds by a different method and loaded with the same amount of active phase is out of the aim of this work and it will require further investigation.

3.3. Used catalysts

The morphology of the samples after catalytic tests was investigated by SEM and EDS analyses. The used RhexHT-1.2 catalyst is formed by flakes of catalyst and many cracks (Fig. 7); furthermore, some catalyst appeared detached during catalytic tests. The flakes are compact and EDS analyses indicate that they are mainly composed by Al and Rh, with a relatively low Mg-content, such as observed for the fresh catalyst. Small particles are observed in the cracks, which may be related to the formation of alumina, although, EDS and backscattering images point to the additional presence of Rh. Furthermore, some carbon nanotubes and amorphous carbon are detected both in the catalyst and in a larger amount, on

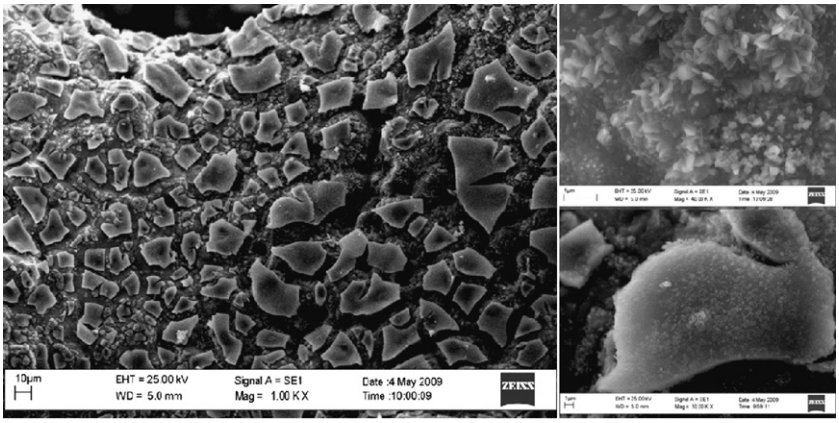

Fig. 7. SEM images at different magnification of the used RhexHT-1.2 catalyst obtained from a HT precursor prepared at −1.2 V for 1000 s without adjusting the pH of the plating solution.

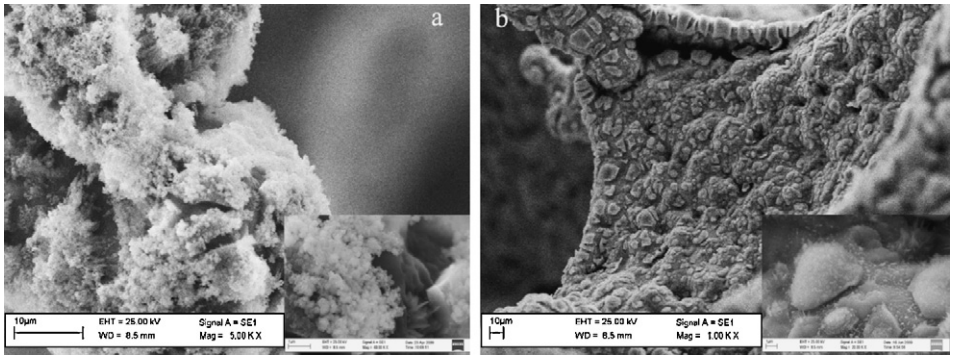

Fig. 8. SEM images of the used RhexHT-1.2 pH (a) and RhexHT-1.3pH (b) catalysts obtained from HT precursors prepared for 1000 s at −1.2 V and −1.3 V, respectively, controlling the pH of the plating solution at 3.8. Insight: high magnification.

the foam surface. SEM images of the spent RhexHT-1.2pH catalyst show that the morphology of the original catalyst film is mainly retained (Fig. 8a). In the uncovered zones, already observed in the fresh sample, EDS analyses reveal a small carbon content. Finally, for the catalyst with the best performances, i.e. that obtained at −1.3 V for 1000 s (Fig. 8b), the cracks are not propagated thus indicating a high adhesion of the coating to the surface; furthermore, Rh particles are observed in the catalyst flakes. Some morphological differences, however, are observed as a function of the section of the catalyst, that may be related to their position in the catalytic bed or to differences in the morphology of the catalyst during the preparation [19,28]. Part of the foam pellets placed in the inlet of the catalytic bed is exposed to high temperatures, leading to the sintering of the rhodium particles and the formation of creeps in the catalytic film. Because lower temperatures are reached close to the outlet, the morphology of the film may be retained.

By taking into account the characterization of the catalysts before and after the catalytic tests as well as the catalytic results, it may be stated that the performances of the structured catalysts are strongly related to the amount of active phase, homogeneity and stability of the catalytic coating. The good performance of the catalyst obtained from the HT precursor at −1.2 V without controlling the pH may be ascribed to a large Rh amount, despite the low stability of the catalytic layer. Likewise, the poor activity of the catalyst prepared under the same synthesis conditions, but adjusting the pH of the plating solution may be related to both the lower Rh content and the poor foam coverage by the catalyst. Finally, the best performances and stability of the catalyst prepared by applying the higher cathodic potential (−1.3 V) may be attributed to a larger Rh amount, better dispersion and higher interaction between support and catalyst as well as, inside this latter, between Rh metal particles and the oxide matrix. The results reported here point out that the electrochemical synthesis may be considered a promising route for the deposition of catalytic coatings on metallic supports. The main advantages of electrosynthesis are: (1) simple and inexpensive equipment is required, (2) films may be obtained on large and irregular surfaces, (3) the deposition occurs closer to equilibrium than with methods using higher temperatures, (4) inter-element diffusion is not a problem, and (5) last but not least, the process may be easily controlled due to its electrical nature. Further studies are in progress to improve the homogeneity of the film.

4. Conclusions

The electrosynthesis of HT precursors on metallic supports is a promising alternative to obtain Rh-based structured catalysts with good performances in the CPO of methane. The chemical nature and morphology of the coating, as well as the degree of coverage of the metallic foam, depend on the pH of the plating solution and potential applied. Consequently, also the catalytic performances (methane conversion and syngas selectivity) are strongly related to the synthesis parameters. The control of the pH of the plating solution (2.1 or 3.8) plays a key role in the formation of HT phases *vs* the Rh^{3+} reduction, whereas the potential applied (−1.2 or −1.3 V) determined the amount of electrosynthesized HT precursors and the coverage of the foam. By increasing the potential applied from −1.2 to −1.3 V a thicker catalyst layer is obtained, although it is more exposed to cracks. Catalytic results show the key role of Rh load in the development of new catalysts, which are able to compete with conventional pelletized catalysts. In this perspec-

tive, the catalyst obtained from an electrosynthesized HT precursor prepared at −1.3 V for 1000 s shows the best catalytic activity and selectivity, associated with good stability with time-on-stream.

Acknowledgement

Financial support from the Ministero per l'Istruzione, Università e Ricerca (MIUR, Roma) is gratefully acknowledged. The authors acknowledge to Prof. M. Gazzano for his help in the XRD measurements.

References

[1] A.P.E. York, T. Xiao, M.L.H. Green, Top. Catal. 22 (2003) 345.
[2] T.V. Choudhary, V.R. Choudhary, Angew. Chem. Int. Ed. 47 (2008) 1828.
[3] J.D. Holladay, J. Hu, D.L. King, Y. Wang, Catal. Today 139 (2009) 244.
[4] B.C. Enger, R. Lødeng, A. Holmen, Appl. Catal. A 346 (2008) 1.
[5] A. Cybulski, J.A. Moulijn (Eds.), Structured Catalysts and Reactors, CRC Taylor & Francis, Boca Raton (USA), 2005.
[6] L. Bobrova, N. Vernikovskaya, V. Sadykov, Catal. Today 144 (2009) 185.
[7] P.O. Sharma, M.A. Abraham, S. Chattopadhay, Ind. Eng. Chem. Res. 46 (2007) 9053.
[8] K.H. Hofstad, O.A. Rokstad, A. Holmen, Catal. Lett. 36 (1996) 25.
[9] K. Heitnes, S. Lindberg, O.A. Rokstad, A. Holmen, Catal. Today 24 (1995) 211.
[10] D.A. Hickman, L.D. Schmidt, J. Catal. 138 (1992) 267.
[11] Y.P. Tulenin, M.Y. Sinev, V.V. Savkin, V.N. Korchak, Catal. Today 91–92 (2004) 155.
[12] L.J.I. Coleman, E. Croiset, W. Epling, M. Fowler, R.R. Hudgins, Catal. Lett. 128 (2009) 144.
[13] D.A. Hickman, E.A. Haupfear, L.D. Schmidt, Catal. Lett. 17 (1993) 223.
[14] D. Dalle Nogare, N.J. Degenstein, R. Horn, P. Canu, L.D. Schmidt, J. Catal. 258 (2008) 131.
[15] A. Bitsch-Larsen, R. Horn, L.D. Schmidt, Appl. Catal. A 348 (2008) 165.
[16] A. Donazzi, B.C. Michael, L.D. Schmidt, J. Catal. 260 (2008) 270.
[17] C.J. Bell, C.A. Leclerc, Energy Fuels 21 (2007) 3548.
[18] R. Horn, K.A. Williams, N.J. Degenstein, A. Bitsch-Larsen, D. Dalle Nogare, S.A. Tupy, L.D. Schmidt, J. Catal. 249 (2007) 380.
[19] S. Ding, Y. Yang, Y. Jin, Y. Cheng, Ind. Eng. Chem. Res. 48 (2009) 2878.
[20] S. Cimino, R. Torbati, L. Lisi, G. Russo, Appl. Catal. A 360 (2009) 43.
[21] K. Heitnes, S. Lindberg, O.A. Rokstad, A. Holmen, Catal. Today 21 (1994) 471.
[22] A. Beretta, G. Groppi, M. Lualdi, I. Tavazzi, P. Forzatti, Ind. Eng. Chem. Res. 48 (2009) 3825.
[23] R. Schwiedernoch, S. Tischer, C. Correa, O. Deutschmann, Chem. Eng. Sci. 58 (2003) 633.
[24] T. Liu, C. Snyder, G. Veser, Ind. Eng. Chem. Res. 46 (2007) 9045.
[25] A. Bitsch-Larsen, N.J. Degenstein, L.D. Schmidt, Appl. Catal. B: Environ. 78 (2007) 364.
[26] N.N. Sazonova, S.N. Pavlova, S.A. Pokrovskaya, N.A. Chumakova, V.A. Sadykov, Chem. Eng. J. 154 (2009) 17.
[27] T. Sanders, P. Papas, G. Veser, Chem. Eng. J. 142 (2008) 122.
[28] B.C. Enger, J. Walmsley, E. Bjørgum, R. Lødeng, P. Pfeifer, K. Schubert, A. Holmen, H.J. Venvik, Chem. Eng. J. 144 (2008) 489.
[29] H. Jung, W.L. Yoon, H. Lee, J.S. Park, J.S. Shin, H. Lab, J.D. Leehave, J. Power Sources 124 (2003) 76.
[30] J.-H. Ryu, K.-Y. Lee, H.-J. Kim, J.-I. Yang, H. Jung, Appl. Catal. B: Environ. 80 (2008) 306.
[31] A. Shamsi, J.J. Spivey, Ind. Eng. Chem. Res. 44 (2005) 7298.
[32] U. Zavyalova, F. Girgsdies, O. Korup, R. Horn, R. Schlögl, J. Phys. Chem. C113 (2009) 17493.
[33] E. Arendt, A. Maione, A. Klisinska, O. Sanz, M. Montes, S. Suarez, J. Blanco, P. Ruiz, J. Phys. Chem. C113 (2009) 16503.
[34] B.P. Barbero, L. Costa-Almeida, O. Sanz, M.R. Morales, L.E. Cadus, M. Montes, Chem. Eng. J. 139 (2008) 430.
[35] L. Giani, C. Cristiani, G. Groppi, E. Tronconi, Appl. Catal. B: Environ. 62 (2006) 121.
[36] L. Indira, P.V. Kamath, J. Mater. Chem. 4 (1994) 1487.
[37] G.H.A. Therese, P.V. Kamath, Chem. Mater. 12 (2000) 1195.
[38] D.-R. Kim, K.-W. Cho, Y.-I. Choi, C.-J. Park, Int. J. Hydrogen Energy 34 (2009) 2622.
[39] M. Gupta, J.J. Spivey, Catal. Today 147 (2009) 126.
[40] T. Novaković, N. Radi, B. Grbić, T. Marinova, P. Stefanov, D. Stoychev, Catal. Commun. 9 (2008) 1111.
[41] D. Gary, P. Del Gallo, F. Basile, G. Fornasari, V. Rosetti, A. Vaccari, E. Scavetta, D. Tonelli, Eur. Pat. Appl. EP 1,808,229 A1 (2007) To Air Liquide.
[42] F. Basile, P. Benito, P. Del Gallo, G. Fornasari, D. Gary, V. Rosetti, E. Scavetta, D. Tonelli, A. Vaccari, Chem. Commun. (2008) 2917.
[43] F. Basile, P. Benito, G. Fornasari, V. Rosetti, E. Scavetta, D. Tonelli, A. Vaccari, Appl. Catal. B: Environ. 91 (2009) 563.
[44] F. Cavani, F. Trifirò, A. Vaccari, Catal. Today 11 (1991) 173.
[45] A. Vaccari, Catal. Today 41 (1998) 53.
[46] S. Albertazzi, F. Basile, A. Vaccari, in: F. Wypych (Ed.), Clay Surfaces: Fundamentals and Applications, Elsevier, Amsterdam (NL), 2004, p. 497.
[47] F. Basile, S. Albertazzi, D. Gary, G. Fornasari, A. Vaccari, P. Arpentinier, WO Pat. Appl. 03,099,436 (2003) To Air Liquide.
[48] F. Basile, G. Fornasari, M. Gazzano, A. Kiennemann, A. Vaccari, J. Catal. 217 (2003) 245.
[49] F. Basile, P. Benito, G. Fornasari, A. Vaccari, Appl. Clay Sci. 48 (2010) 250.
[50] E. Scavetta, A. Mignani, D. Prandstraller, D. Tonelli, Chem. Mater. 19 (2007) 4523.
[51] M. Pourbaix, Atlas d'equilibres thermodinamiques a 25 °C, Gauthier-Villars, Paris (F), 1963.
[52] R. Chegroune, E. Salhi, A. Crisci, Y. Wouters, A. Galerie, Oxid. Met. 70 (2008) 331.
[53] Y. Hamlaoui, F. Pedraza, L. Tifouti, Corros. Sci. 50 (2008) 2182.
[54] C. Agrafiotis, A. Tsetsekou, J. Eur. Ceram. Soc. 20 (2000) 815.
[55] C.-P. Hwang, C.-T. Yeha, Q. Zhu, Catal. Today 51 (1999) 93.
[56] M. Maestri, D.G. Vlachos, A. Beretta, G. Groppi, E. Tronconi, J. Catal. 259 (2008) 211.
[57] A. Donazzi, A. Beretta, G. Groppi, P. Forzatti, J. Catal. 225 (2008) 241.
[58] F. Basile, L. Basini, M. D' Amore, G. Fornasari, A. Guarinoni, D. Matteuzzi, G. Del Piero, F. Trifirò, A. Vaccari, J. Catal. 173 (1998) 247.
[59] F. Basile, P. Benito, G. Fornasari, D. Gazzoli, I. Pettiti, V. Rosetti, A. Vaccari, Catal. Today 142 (2009) 78.
[60] F. Basile, G. Fornasari, F. Trifirò, Stud. Surf. Sci. Catal. 130 (2000) 449.
[61] F. Basile, G. Fornasari, F. Trifrò, A. Vaccari, Catal. Today 64 (2001) 21.